

Original articles

Research article

<https://doi.org/10.17308/kcmf.2025.27/13329>

Study of the influence of the microstructure of Pt/C materials on the electrochemical characteristics of PtCo/C electrocatalysts based on them

A. K. Nevelskaya^{1,2✉}, S. V. Belenov¹, A. A. Gavrilova¹, K. O. Paperzh¹,
N. V. Lyanguzov³, I. V. Pankov⁴, A. A. Kokhanov¹

¹Southern Federal University, Faculty of Chemistry,
7 ul. Sorge, Rostov-on-Don 344090, Russian Federation

²Federal Research Center Southern Scientific Center of the Russian Academy of Sciences (SSC RAS),
41 pr. Chekhov, Rostov-on-Don 344006, Russian Federation

³Southern Federal University, Faculty of Physics,
5 ul. Sorge, Rostov-on-Don 344090, Russian Federation

⁴Southern Federal University, Research Institute of Physical and Organic Chemistry,
194/2 pr. Stachki, Rostov-on-Don 344090, Russian Federation

Abstract

Objectives: The paper studies the effect of the uniformity of spatial distribution of Pt nanoparticles over the support surface in Pt/C materials on the microstructure and electrochemical behavior of PtCo/C catalysts obtained on their basis. PtCo/C catalysts are synthesized by the impregnation of Pt/C followed by heat treatment in an Ar/H₂ atmosphere. The use of a Pt/C material with a platinum mass fraction of about 20% and a uniform distribution of Pt nanoparticles over the surface of the carbon support makes it possible to obtain a PtCo/C catalyst, the activity of which in the oxygen reduction reaction at 0.90 V is 1215 A/g (Pt), which is 4.8 times higher than a similar figure for a commercial Pt/C catalyst. In this case, the use of a Pt/C material with an ununiform distribution of nanoparticles leads to the production of a PtCo/C catalyst with large particle size and low active surface area, which significantly worsens its activity in oxygen reduction reactions. The purpose of this article is to study the effect of the uniformity of the spatial distribution of Pt nanoparticles over the support surface in Pt/C materials on the microstructure and electrochemical behavior of the PtCo/C catalysts obtained from them.

Experimental: PtCo/C catalysts were synthesized by impregnation with Pt/C followed by heat treatment in an Ar/H₂ atmosphere.

Conclusions: The use of a Pt/C material with a platinum content of approximately 20% and a uniform distribution of Pt nanoparticles over the carbon support surface allows the production of a PtCo/C catalyst with an oxygen reduction reaction (ORR) activity of 1215 A/g (Pt) at 0.90 V, which is 4.8 times higher than that of a commercial Pt/C catalyst. The use of a Pt/C material with a non-uniform distribution of nanoparticles results in a PtCo/C catalyst with a large particle size and a low active surface area, which significantly reduces its ORR activity.

Keywords: Platinum-based electrocatalysts, Bimetallic nanoparticles, High-temperature synthesis, Heat treatment, Oxygen electroreduction reaction

Funding: This research conducted at the Southern Federal University was financially supported by the Russian Science Foundation (Grant No. 24-79-00279).

Acknowledgement: The authors are also grateful to the Shared Use Center “High-Resolution Transmission Electron Microscopy” (SFedU) for conducting the TEM studies.

For citation: Nevelskaya A. K., Belenov S. V., Gavrilova A. A., Paperzh K. O., Lyanguzov N. V., Pankov I. V., Kokhanov A. A. Study of the influence of the microstructure of Pt/C materials on the electrochemical characteristics of PtCo/C electrocatalysts based on them. *Condensed Matter and Interphases*. 2025;27(4): 651–660. <https://doi.org/10.17308/kcmf.2025.27/13329>

✉ Alina K. Nevelskaya, e-mail: alina_nevelskaya@mail.ru

© Nevelskaya A. K., Belenov S. V., Gavrilova A. A., Paperzh K. O., Lyanguzov N. V., Pankov I. V., Kokhanov A. A., 2025



The content is available under Creative Commons Attribution 4.0 License.

Для цитирования: Невельская А. К., Беленов С. В., Гаврилова А. А., Паперж К. О., Лянгузов Н. В., Панков И. В., Коханов А. А. Изучение влияния микроструктуры Pt/C материалов на электрохимические характеристики полученных на их основе PtCo/C электрокатализаторов. *Конденсированные среды и межфазные границы*. 2025;27(4): 651–660. <https://doi.org/10.17308/kcmf.2025.27.13329>

1. Introduction

Finding ways to enhance the activity and stability of platinum-based electrocatalysts is a critical task for advancing various areas of hydrogen energy, such as low-temperature fuel cells (LTFCs) [1–4]. One effective approach involves doping platinum with d-metals (e.g., Co, Ni, Fe, Cu) [5–7]. By varying the composition and structure of the resulting nanoparticles, this strategy can improve the functional characteristics of the catalyst [8–14] while reducing its cost.

It is known that a catalyst's performance is largely determined by its morphology, including the distribution of metal nanoparticles on the carbon support, as well as their shape, composition, structure, average size, and size distribution [15–18]. Furthermore, catalysts incorporating bimetallic nanoparticles often exhibit enhanced stability due to stronger metal-support interactions. Therefore, for bimetallic systems, these factors must be carefully considered when developing an optimal synthesis strategy.

Among various candidates, PtCo/C catalysts are regarded as the most promising for LTFCs, combining high activity in the oxygen reduction reaction (ORR) with outstanding stability [4, 19, 20]. The high practical relevance of research on PtCo/C catalysts is underscored by their application in commercial systems, such as the Toyota Mirai fuel cell [21].

The functional properties of bimetallic catalysts are determined by the chemical composition and structure of their nanoparticles, as well as by the distribution of these particles on the carbon support. For instance, achieving a high degree of alloying in PtCo/C catalyst nanoparticles is crucial. Cobalt atoms that are not incorporated into the platinum lattice can dissolve during operation and poison the polymer electrolyte membrane, thereby degrading the performance of the LTFC [22]. However, incorporating Co atoms into the Pt nanoparticles during synthesis

is challenging. In many cases, subsequent heat treatment is required, which can lead to particle agglomeration (coarsening), a reduction in active surface area, and consequently, a loss of catalytic activity. Furthermore, forming bimetallic PtCo nanoparticles with an ordered alloy structure (an intermetallic phase) can significantly enhance the catalyst's stability compared to materials with a disordered alloy structure [22, 24].

High-temperature synthesis in a reducing atmosphere is a promising route for producing platinum-based electrocatalysts for low-temperature fuel cells, offering advantages such as high-performance characteristics. Several methods exist for the high-temperature synthesis of bimetallic platinum catalysts.

The first approach involves impregnating a high-surface-area carbon support with precursors of platinum and a d-metal in the required ratio, followed by carbothermic reduction in an inert atmosphere with hydrogen [25–27]. The uniformity of the final product depends heavily on the properties of the carbon support and the high-temperature reduction conditions. Another method utilizes a pre-synthesized Pt/C catalyst (often commercial), which is impregnated with a d-metal precursor. Subsequent heat treatment in an inert atmosphere with a small amount of hydrogen reduces the metal oxide/hydroxide and facilitates its “fusion” with platinum nanoparticles [28, 29]. In this case, the properties of the resulting bimetallic catalyst are determined not only by the temperature and atmosphere but also by the microstructure of the initial Pt/C material.

While several studies have investigated the effects of temperature and atmosphere on the properties of PtM/C catalysts prepared by this method, systematic studies on the influence of the Pt/C precursor's microstructure are lacking. This includes the role of the average size and size distribution of platinum nanoparticles, as well as their dispersion on the carbon support, on the structural characteristics

and electrochemical performance of the final bimetallic catalysts.

Therefore, the aim of this work was to prepare a series of PtCo/C catalysts via high-temperature treatment in a reducing atmosphere using Pt/C precursors with varying microstructures, and to conduct a comparative study of the composition, structure, and catalytic activity of the resulting materials in the oxygen reduction reaction.

2. Experimental

2.1. Deposition of Co(OH)_2 on a Pt/C catalyst

The development of highly efficient catalysts containing non-precious metals is an important and promising area of hydrogen energy research. The synthesis method described herein allows for the production of catalysts exhibiting high activity in ORR and enhanced stability.

A sample of a Pt/C catalyst (with a Pt loading of approximately 20 wt. %) was placed in a beaker, and 60 mL of ethylene glycol (reagent grade, AO "EKOS-1", Moscow, Russia) measured with a cylinder was added. A magnetic stir bar was placed into the resulting suspension, and it was stirred on a magnetic stirrer for 2–3 minutes. Subsequently, the mixture was subjected to ultrasonic dispersion twice for 2 minutes each (using an Ultrasonic Processor FS-1200N) and then returned to the magnetic stirrer. A calculated volume of the cobalt precursor, $\text{CoSO}_4 \cdot 7\text{H}_2\text{O}$, as an aqueous solution with a concentration of 0.071 M, was added via a dispenser, and stirring was continued for 1 hour [30].

Following this, a calculated amount of NaOH, dissolved in 20 mL of bidistilled water, was introduced to precipitate cobalt hydroxide. The mixture was stirred on a magnetic stirrer for another hour. The catalyst suspension was filtered using a Büchner funnel with "Blue Ribbon" filter paper and washed sequentially with water, ethanol, and again with water, each for at least three cycles. The catalyst on the filter was then dried at 80 °C in a vacuum oven. After drying, the catalyst was separated from the filter paper, and the resulting powder was subjected to thermal treatment in a tube furnace at 700 °C

for 1 hour under a flow of inert gas containing 5 % hydrogen.

Two types of Pt/C catalysts were used to prepare the bimetallic catalysts: (1) a catalyst with a uniform distribution of nanoparticles on the Vulcan XC-72 carbon support (Fig. 1a), designated as Pt/C-u, which is characterized by a high electrochemical active surface area (ECSA) of $80 \text{ m}^2/\text{g(Pt)}$; and (2) a catalyst with a non-uniform distribution, a high fraction of agglomerates (Fig. 1b), and an ECSA of $25 \text{ m}^2/\text{g(Pt)}$, designated as Pt/C-n. After thermal treatment at 700 °C, the samples were labeled as PtCo/C-u and PtCo/C-n, respectively, according to the type of Pt/C material used.

2.2. Investigation of the composition and structure of PtCo/C catalysts

The phase composition of the obtained materials was studied on an ARL X'TRA diffractometer ($\text{CuK}\alpha$) in the 2θ range from 15° to 55° with a step of 0.04° and a recording rate of 2° per minute. The elemental composition of the materials was studied by X-ray fluorescence analysis on an RFS-001 spectrometer with total internal reflection (TXRF). The average size, shape, and spatial distribution of nanoparticles on the surface of the carbon support were studied using a JEM-F200 transmission electron microscope (TEM) (JEOL). A JEOL EM-01361RSTHB beryllium sample holder with a double tilt was used for TEM measurements. TEM images were obtained at magnifications from $30000\times$ to $600000\times$.

2.3. Electrochemical characterization

The electrochemical behavior of the electrocatalysts was studied using a three-electrode cell and a rotating disk electrode (RDE) in a 0.1 M HClO_4 electrolyte [31]. Catalytic ink was prepared by dispersing 0.006 g of the catalyst in a mixture of 2000 μL isopropyl alcohol and 40 μL of a 5 wt. % Nafion solution via 30-minute ultrasonication to form a homogeneous suspension. A calculated aliquot of the ink was drop-cast onto a glassy carbon disk electrode to achieve a uniform Pt loading of $19\text{--}21 \mu\text{g/cm}^2$.

Standardization of the electrode surface and recording of cyclic voltammograms (CVs) to determine the ECSA were performed according to the procedure described in [31]. The activity of

the synthesized catalysts in ORR was evaluated by voltammetry with a linear potential sweep on a rotating disk electrode. The kinetic current was calculated at a potential of 0.90 V using the Koutecky–Levich equation [31]. All potentials in this work are given relative to a reversible hydrogen electrode (RHE).

3. Results and discussion

Two Pt/C materials with distinct microstructures were selected for cobalt doping: (1) Pt/C-u with a uniform distribution of nanoparticles on the carbon support surface (Fig. 1) and an average crystallite size of approximately 2.3 nm (Table 1); and (2) Pt/C-n, a material with a non-uniform nanoparticle distribution, pronounced agglomeration, and a slightly larger average crystallite size of 3.0 nm, as determined by X-ray diffraction (XRD) analysis.

It should be noted that despite using the same amount of cobalt precursors (calculated for a Pt:Co atomic ratio of 1:1) deposited on the Pt/C materials, the composition of the resulting PtCo/C materials differed depending on the synthesis methodology. When cobalt precursors

were deposited onto the Pt/C-u material using an alkali, the composition of the resulting catalyst was Pt_1Co_1 , which corresponds to the atomic ratio of the precursors used in the synthesis. In contrast, for the PtCo/C-n catalyst derived from the Pt/C-n material, the composition corresponded to $\text{PtCo}_{1.6}$. This indicates that the PtCo/C-n catalyst contained a lower proportion of Pt compared to the PtCo/C-u material, which may be attributed to specific features of the synthesis procedure and metal losses during the process. The platinum mass fraction in the PtCo/C-n material was 14 % (Table 1), which is lower than expected from the precursor loading and supports the assumption of metal losses during synthesis.

During the deposition of cobalt onto a Pt/C support followed by thermal treatment in an inert atmosphere, two primary processes can occur: the formation of bimetallic PtCo nanoparticles via atomic diffusion, and the coarsening of metal nanoparticles through agglomeration.

The formation of bimetallic nanoparticles after the deposition of cobalt precursors on Pt/C materials and subsequent thermal treatment is

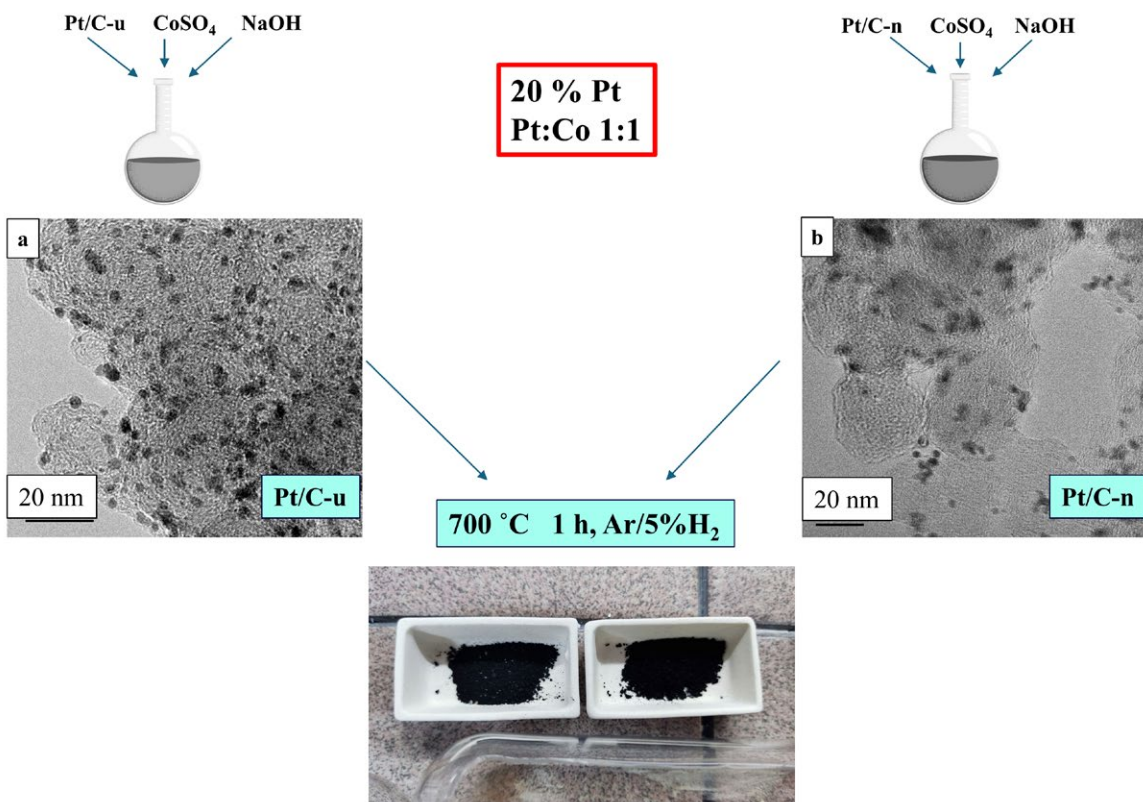


Fig. 1. Synthesis scheme of PtCo/C catalysts on various Pt/C materials

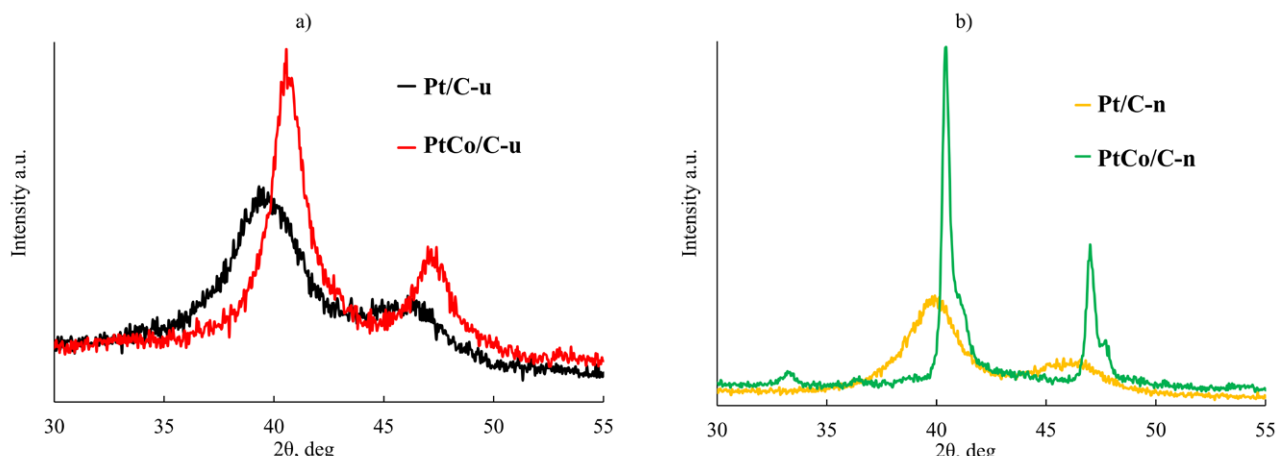
Table 1. Structural characteristics of PtCo/C catalysts obtained on the basis of various Pt/C materials

Sample	$\omega(\text{Pt})$, %	Composition TXRF	Lattice parameter, Å	Composition XRD	Average crystallite size, nm
Pt/C-p	21±1	Pt	3.94(6)	–	2.3±0.2
	18±1	Pt	3.93(3)	–	3.0±0.2
PtCo/C-p	18±1	$\text{PtCo}_{1.0}$	3.85(3)	$\text{PtCo}_{0.23}$	4.5±0.2
	14±1	$\text{PtCo}_{1.6}$	3.86(6) 3.81(1)	$\text{PtCo}_{0.18}$ $\text{PtCo}_{0.44}$	30±3 10±1

confirmed by XRD data. A shift of the reflections corresponding to the face-centered cubic (fcc) structure of platinum towards higher 2θ angles was observed (Fig. 2a). This indicates a decrease in the crystal lattice parameter (Table 1) due to the formation of an alloy of platinum with cobalt. The extent of the peak shift and the phase composition of the resulting PtCo/C catalysts depend on the type of Pt/C material used. For the PtCo/C-u catalyst, derived from the uniformly distributed Pt/C material, a single PtCo phase with a lattice parameter of 3.853 Å was formed. In contrast, XRD analysis of the PtCo/C-n catalyst revealed two distinct metallic phases (Table 1). The composition of the Pt-Co alloy can be estimated from the lattice parameter using Vegard's law. For the PtCo/C-n material, the compositions are $\text{PtCo}_{0.18}$ and $\text{PtCo}_{0.44}$ for the phases with lower and higher cobalt content, respectively. A discrepancy was noted between the composition of the bimetallic phases

determined by XRD and the bulk composition from elemental analysis. This suggests that not all cobalt is incorporated into the platinum lattice to form an alloy. The cobalt not alloyed with platinum may exist in the material as a separate phase, likely an X-ray amorphous cobalt oxide or hydroxide. Analysis of the average crystallite size in the bimetallic catalysts using the Scherrer equation [31] showed that thermal treatment leads to different structural changes in the materials. For the PtCo/C-u catalyst, a slight increase in nanoparticle size to 4.5 nm was observed. Conversely, the PtCo/C-n material exhibited more significant particle coarsening, with sizes reaching 10–30 nm.

Furthermore, additional reflections appeared on the XRD pattern of the PtCo/C-n material after thermal treatment. The presence of these reflections may indicate the formation of Pt-Co intermetallic compounds. However, their low intensity makes precise identification

**Fig. 2.** X-ray diffraction patterns of Pt/C materials and PtCo/C catalysts obtained on their basis with uniform (a) and non-uniform (b) distribution of nanoparticles over the surface of the carbon support

difficult.

According to TEM data (Fig. 3), the PtCo/C-u catalyst is characterized by a uniform distribution of metal nanoparticles on the carbon support surface. TEM results also revealed that the material contains nanoparticles with a size range of 2 to 8 nm (Fig. 3b), as well as large nanoparticle agglomerates up to 30 nm in size (Fig. 3b). A particle size distribution histogram was constructed based on the analysis of TEM images (Fig. 3c), and the average size of the metal nanoparticles was calculated to be 4.7 nm. The histogram shows a wide dispersion, indicating the presence of both small nanoparticles (around 2 nm) and larger ones exceeding 8 nm. It is important to note that the large nanoparticle agglomerates were not included in the calculation of the average particle size or in the construction of the histogram due to methodological constraints in their accurate accounting. The average nanoparticle size for the PtCo/C-u material, as determined by TEM, closely matches the average crystallite size of PtCo calculated using the Scherrer equation (Table 1). Thus, the bimetallic catalyst derived from the uniform Pt/C material exhibits a uniform distribution of nanoparticles across the carbon support surface but simultaneously possesses a very broad particle size distribution and the presence of agglomerates, which is a detrimental factor for developing highly efficient catalysts. Consequently, further optimization of the cobalt precursor deposition method and thermal

treatment conditions is likely required to obtain a catalyst with a narrower size distribution.

Evaluation of the ECSA by cyclic voltammetry (Fig. 4) revealed significant differences between the PtCo/C materials derived from Pt/C precursors with different uniformities. The ECSA for the PtCo/C-u material was about $50 \text{ m}^2/\text{g(Pt)}$ (Table 2), which is somewhat lower than that of the commercial Pt/C analogue (ECSA = $84 \text{ m}^2/\text{g(Pt)}$). This decrease is likely associated with the larger size and broader size distribution of the nanoparticles in the bimetallic material. Notably, the deposition of cobalt followed by thermal treatment led to a reduction in the ECSA for the PtCo/C-u material compared to the original Pt/C-u (Table 2), which can be attributed to particle growth during the high-temperature synthesis of the bimetallic catalyst. The ECSA for the PtCo/C-n material, derived from the non-uniform Pt/C precursor, was significantly lower than that of PtCo/C-u. This can be explained both by the lower initial ECSA of the Pt/C-n precursor and the larger metal particle size in the final PtCo/C-n material (Table 1).

The polarization curves in Fig. 4 exhibit a typical shape for platinum-based catalysts. From 1.10 V to an onset potential of about 0.98 V for PtCo/C-n and Pt/C, and about 1.00 V for PtCo/C-u (Fig. 4c, Region I; Fig. 4d), the current is zero, indicating that the ORR does not proceed. Upon reaching the onset potential, the cathodic current increases as the potential decreases. This region is independent of the

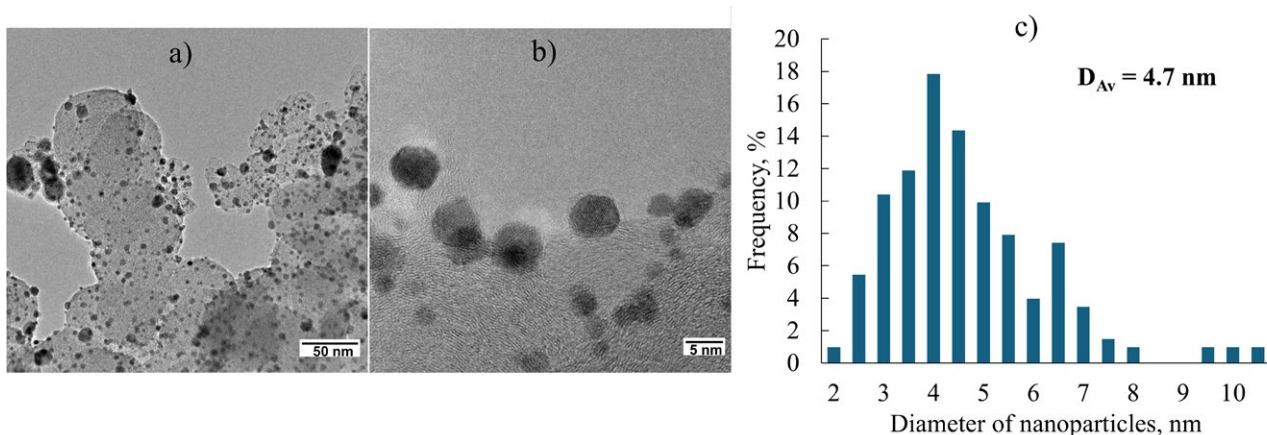


Fig. 3. TEM images (a, b) and histogram of the size distribution of nanoparticles (c) of PtCo/C-u catalyst obtained on the basis of Pt/C catalyst with uniform distribution of nanoparticles

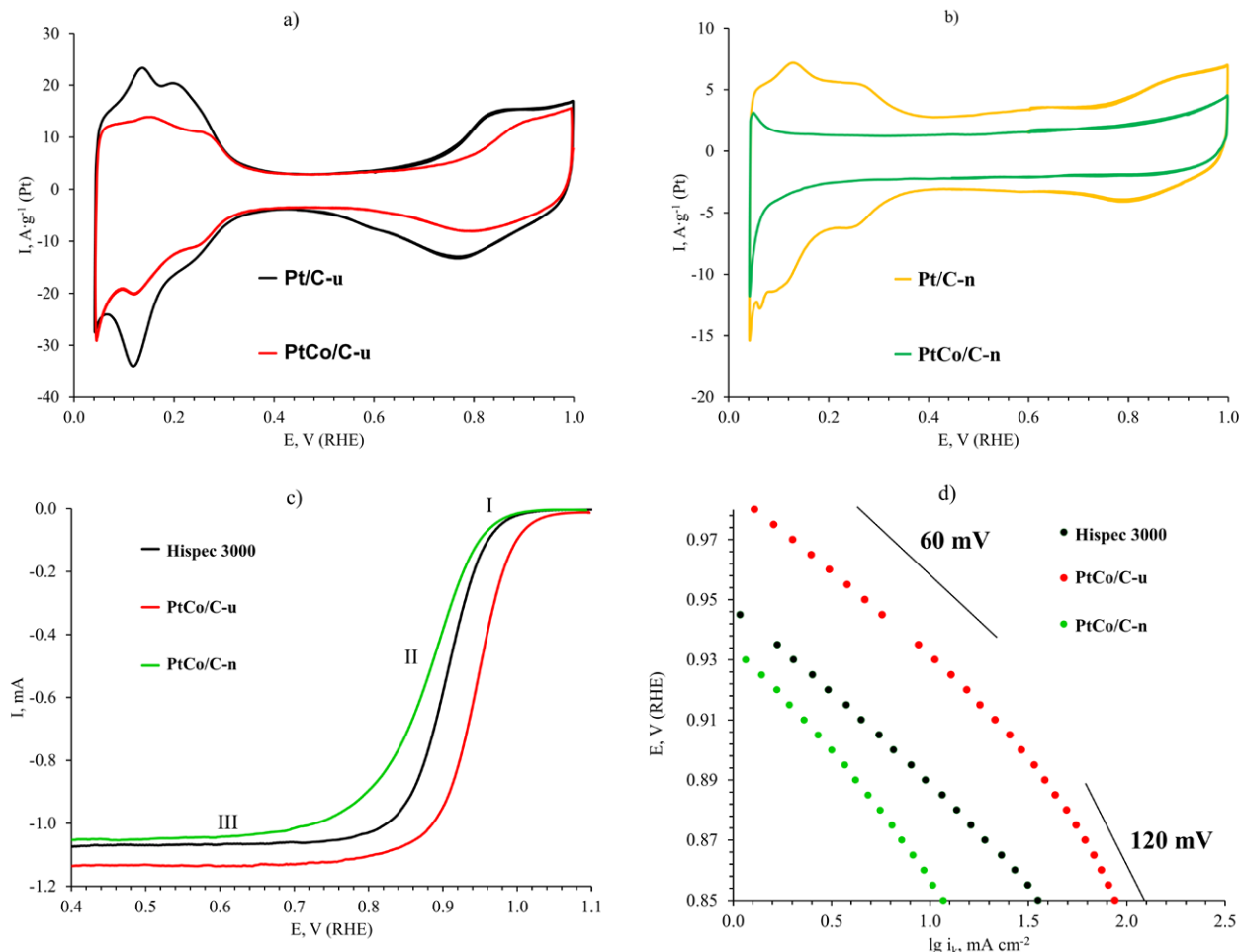


Fig. 4. Cyclic voltammograms of PtCo/C catalysts obtained using various Pt/C catalysts (a, b); linear potential sweep voltammograms (c) and Tafel dependence for the obtained PtCo/C catalysts, as well as the commercial Pt/C catalyst Hispec 3000 (d)

Table 2. Electrochemical characteristics of the obtained PtCo/C catalysts, as well as the commercial Pt/C catalyst Hispec 3000

Sample	ECSA, m^2/g (Pt)	I_k , mA	I_m , A/g (Pt) (at 0.90 V)	I_s , A/m^2 (Pt) (at 0.90 V)	$E_{1/2}$, V
PtCo/C-p	50 ± 5	5.0 ± 0.5	1215 ± 122	24.3 ± 2.4	0.94 ± 0.01
PtCo/C-n	< 3	0.6 ± 0.1	192 ± 19	—	0.88 ± 0.01
Hispec 3000	84 ± 8	1.2 ± 0.1	254 ± 25	3.0 ± 0.3	0.91 ± 0.01

electrode rotation rate, and the reaction rate is governed solely by the sluggish kinetics of the ORR. With a further decrease in potential, oxygen diffusion to the electrode surface begins to contribute. This region (Fig. 4c, Region II) is characterized by mixed kinetic-diffusion control. At even lower potentials, the cathodic current becomes independent of the applied potential as it becomes limited solely by the rate of oxygen

supply to the electrode surface – this is the region of the limiting diffusion current (Fig. 4c, Region III).

The catalytic activity at 0.90 V, normalized both to the mass of Pt (mass activity, I_m), and to the ECSA (specific activity, I_s), demonstrates the superior performance of the PtCo/C-u material. Its mass activity of 1215 A/g(Pt) and specific activity of $24.3 \text{ A/m}^2(\text{Pt})$ far exceed those of the

commercial Pt/C analogue (254 A/g(Pt)), despite its lower ECSA (Table 2). In contrast, the PtCo/C-n material shows significantly lower activity compared to the commercial Pt/C, which can be attributed to its extremely low ECSA. Based on the half-wave potential ($E_{1/2}$), the studied samples can be ranked in the following order of increasing activity: PtCo/C-n < Pt/C < PtCo/C-u. The half-wave potential serves as a key indicator of activity, alongside kinetic current values. Thus, it is confirmed that the PtCo/C-u catalyst, possessing the highest half-wave potential of 0.94 V among all samples, exhibits the greatest activity in the ORR.

4. Conclusions

A study on model Pt/C samples with uniform and non-uniform distributions of platinum nanoparticles demonstrated the decisive influence of this parameter on the performance of the resulting bimetallic PtCo/C catalysts. It was found that the PtCo/C catalyst derived from the uniformly distributed Pt/C precursor exhibits a larger electrochemical surface area and a mass activity more than six times higher than that of the catalyst obtained from the non-uniform Pt/C material. Furthermore, the mass activity of the most active PtCo/C catalyst exceeded that of a commercial Pt/C catalyst by a factor of 4.8.

Thus, the presented high-temperature synthesis method for PtCo/C electrocatalysts has proven to be both promising and scalable for producing highly efficient bimetallic materials. Future work will focus on synthesizing catalysts with varying metal loadings and testing their performance in membrane-electrode assemblies of low-temperature fuel cells.

Contribution of the authors

A. K. Nevelskaya: Investigation, Data curation, Writing - original draft. S. V. Belenov: Supervision, Conceptualization, Writing - review & editing, Project administration. A. A. Gavrilova: Investigation. K. O. Paperzh: Investigation. N. V. Lyanguzov: Investigation. I. V. Pankov: Investigation, TEM analysis. A. A. Kokhanov: Investigation.

Conflict of interests

The authors declare that they have no known competing financial interests or personal relationships that could have influenced the work reported in this paper.

References

- Peng Z, Yang H. Designer platinum nanoparticles: control of shape, composition in alloy, nanostructure and electrocatalytic property. *Nano Today*. 2009;4: 143–164. <https://doi.org/10.1016/j.nantod.2008.10.010>
- Xu G., Yang L., Li J., Liu C., Xing W., Zhu J. Strategies for improving stability of Pt-based catalysts for oxygen reduction reaction. *Advanced Sensor and Energy Materials*. 2023;2: 100058. <https://doi.org/10.1016/j.aseems.2023.100058>
- Xiao F., Wang Y., Wu Z., ... Shao M. Recent advances in electrocatalysts for proton exchange membrane fuel cells and alkaline membrane fuel cells. *Advanced Materials*. 2021;33: 2006292. <https://doi.org/10.1002/adma.202006292>
- Wu D., Shen X., Pan Y., Yao L., Peng Z. Platinum alloy catalysts for oxygen reduction reaction: advances, challenges and perspectives. *ChemNanoMat*. 2020;6: 32–41. <https://doi.org/10.1002/cnma.201900319>
- Wang X. X., Swihart M. T., Wu G. Achievements, challenges and perspectives on cathode catalysts in proton exchange membrane fuel cells for transportation. *Nature Catalysis*. 2019;2: 578–589. <https://doi.org/10.1038/s41929-019-0304-9>
- Glüsen A., Dionigi F., Paciok P., ... Stolten D. Dealloyed PtNi-core–shell nanocatalysts enable significant lowering of Pt electrode content in direct methanol fuel cells. *ACS Catalysis*. 2019;9: 3764–3772. <https://doi.org/10.1021/acscatal.8b04883>
- Jeyabharathi C., Hodnik N., Baldizzone C., ... Mayrhofer K. J. J. Time evolution of the stability and oxygen reduction reaction activity of PtCu/C nanoparticles. *ChemCatChem*. 2013;5: 2627–2635. <https://doi.org/10.1002/cctc.201300287>
- Koh S., Strasser P. Electrocatalysis on bimetallic surfaces: modifying catalytic reactivity for oxygen reduction by voltammetric surface dealloying. *Journal of the American Chemical Society*. 2007;129: 12624–12625. <https://doi.org/10.1021/ja0742784>
- Lopez-Haro M., Dubau L., Guétaz L., ... Maillard F. Atomic-scale structure and composition of $\text{Pt}_3\text{Co}/\text{C}$ nanocrystallites during real PEMFC operation: a STEM–EELS study. *Applied Catalysis B: Environmental*. 2014;152–153: 300–308. <https://doi.org/10.1016/j.apcatb.2014.01.034>
- Gan L., Heggen M., O’Malley R., Theobald B., Strasser P. Understanding and controlling nanoporosity formation for improving the stability of bimetallic fuel cell catalysts. *Nano Letters*. 2013;13: 1131–1138. <https://doi.org/10.1021/nl304488q>
- Lyu X., Jia Y., Mao X., ... Yao X. Gradient-concentration design of stable core–shell nanostructure for acidic oxygen reduction electrocatalysis. *Advanced Materials*. 2020;32: 2003493. <https://doi.org/10.1002/adma.202003493>

14. Gan L., Yu R., Luo J., Cheng Z., Zhu J. Lattice strain distributions in individual dealloyed Pt–Fe catalyst nanoparticles. *The Journal of Physical Chemistry Letters*. 2012;3: 934–938. <https://doi.org/10.1021/jz300192b>

15. Paperzh K. O., Alekseenko A. A., Safronenko O. A., Volochaev V. A., Pankov I. V., Guterman V. E. Stability and activity of platinum nanoparticles in the oxygen electroreduction reaction: is size or ordering of primary importance? 2021: 593–606. <https://doi.org/10.3762/bxiv.2021.27.v1>

16. Paperzh K. O., Pavlets A. S., Alekseenko A. A., Pankov I. V., Guterman V. E. The integrated study of the morphology and the electrochemical behavior of Pt-based ORR electrocatalysts during the stress testing. *International Journal of Hydrogen Energy*. 2023;48: 22401–22414. <https://doi.org/10.1016/j.ijhydene.2023.01.079>

17. Paperzh K., Moguchikh E., Pankov I., Belenov S., Alekseenko A. Effect of AST atmosphere on Pt/C electrocatalyst degradation. *Inorganics (Basel)*. 2023;11: 237. <https://doi.org/10.3390/inorganics11060237>

18. Paperzh K., Alekseenko A., Danilenko M., Pankov I., Guterman V. E. Advanced methods of controlling the morphology, activity, and durability of Pt/C electrocatalysts. *ACS Applied Energy Materials*. 2022;5: 9530–9541. <https://doi.org/10.1021/acsaem.2c01151>

19. Wen Y.-H., Zhang L.-H., Wang J.-B., Huang R. Atomic-scale insights into thermal stability of Pt₃Co nanoparticles: a comparison between disordered alloy and ordered intermetallics. *Journal of Alloys and Compounds*. 2019;776: 629–635. <https://doi.org/10.1016/j.jallcom.2018.10.274>

20. Jung W. S., Popov B. N. Effect of pretreatment on durability of fct-structured Pt-based alloy catalyst for the oxygen reduction reaction under operating conditions in polymer electrolyte membrane fuel cells. *ACS Sustainable Chemistry and Engineering*. 2017;5: 9809–9817. <https://doi.org/10.1021/acssuschemeng.7b01728>

21. Konno N., Mizuno S., Nakaji H., Ishikawa Y. Development of compact and high-performance fuel cell stack. *SAE International Journal of Alternative Powertrains*. 2015;4: 2015-01–1175. <https://doi.org/10.4271/2015-01-1175>

22. Yan W., Sun P., Luo C., ..., Du F. PtCo-based nanocatalyst for oxygen reduction reaction: Recent highlights on synthesis strategy and catalytic mechanism. *Chinese Journal of Chemical Engineering*. 2023;53: 101–123. <https://doi.org/10.1016/j.cjche.2022.03.024>

23. Tong L., Fan L., Liang H.-W. Platinum intermetallic nanoparticle cathode catalysts for proton-exchange-membrane fuel cells: Synthesis and ordering effect. *Current Opinion in Electrochemistry*. 2023;39: 101281. <https://doi.org/10.1016/j.coelec.2023.101281>

24. Liu X., Liang J., Li Q. Design principle and synthetic approach of intermetallic Pt–M alloy oxygen reduction catalysts for fuel cells. *Chinese Journal of Catalysis*. 2023;45: 17–26. [https://doi.org/10.1016/S1872-2067\(22\)64165-2](https://doi.org/10.1016/S1872-2067(22)64165-2)

25. Yang B., Yu X., Hou J., Xiang Z. Secondary reduction strategy synthesis of Pt–Co nanoparticle catalysts towards boosting the activity of proton exchange membrane fuel cells. *Particuology*. 2023;79: 18–26. <https://doi.org/10.1016/j.partic.2022.11.010>

26. Wan K., Wang J., Zhang J., ..., Zhang C. Ligand carbonization in-situ derived ultrathin carbon shells enable high-temperature confinement synthesis of PtCo alloy catalysts for high-efficiency fuel cells. *Chemical Engineering Journal*. 2024;482: 149060. <https://doi.org/10.1016/j.cej.2024.149060>

27. Lima F. H. B., de Castro J. F. R., Santos L. G. R. A., Ticianelli E. A. Electrocatalysis of oxygen reduction on carbon-supported Pt–Co nanoparticles with low Pt content. *Journal of Power Sources*. 2009;190: 293–300. <https://doi.org/10.1016/j.jpowsour.2008.12.128>

28. Mai Y., XIE X., Wang Z., Yan C., Liu G. Effect of heat treatment temperature on the Pt3Co binary metal catalysts for oxygen reduced reaction and DFT calculations. *Journal of Fuel Chemistry and Technology*. 2022;50: 114–121. [https://doi.org/10.1016/S1872-5813\(21\)60099-3](https://doi.org/10.1016/S1872-5813(21)60099-3)

29. Koh S., Hahn N., Yu C., Strasser P. Effects of composition and annealing conditions on catalytic activities of dealloyed Pt–Cu nanoparticle electrocatalysts for PEMFC. *Journal of The Electrochemical Society*. 2008;155: B1281. <https://doi.org/10.1149/1.2988741>

30. Belenov S., Mauer D., Moguchikh E...Alekseenko A. New approach to synthesizing cathode PtCo/C catalysts for low-temperature fuel cells. *Nanomaterials*. 2024;14: 856. <https://doi.org/10.3390/nano14100856>

31. Belenov S., Nevelskaya A., Nikulin A., Tolstunov M. The effect of pretreatment on a PtCu/C catalyst's structure and functional characteristics. *International Journal of Molecules*. 2023;24: 2177. <https://doi.org/10.3390/ijms24032177>

Information about the authors

Alina K. Nevelskaya, Cand. Sci. (Chem.), Researcher at the Department of Electrochemistry, Southern Federal University (Rostov-on-Don, Russian Federation); Junior Researcher at the Federal Research Center Southern Scientific Center of the Russian Academy of Sciences (SSC RAS) (Rostov-on-Don, Russian Federation).

<https://orcid.org/0000-0001-5799-9925>
alina_nevelskaya@mail.ru

Sergey V. Belenov, Cand. Sci. (Chem.), Leading Researcher at the Department of Electrochemistry, Faculty of Chemistry, Southern Federal University (Rostov-on-Don, Russian Federation).

<https://orcid.org/0000-0003-2980-7089>
serg1986chem@mail.ru

Anna A. Gavrilova, student, Research Intern, Southern Federal University (Rostov-on-Don, Russian Federation).

<https://orcid.org/0009-0006-7596-6821>
ganna2800@mail.ru

Kirill O. Paperzh, Junior Researcher at the Department of Electrochemistry, Southern Federal University (Rostov-on-Don, Russian Federation).

<https://orcid.org/0000-0003-4878-9728>
paperzh@sfedu.ru

Nikolay V. Lyanguzov, Cand. Sci. (Chem.), Associate Professor of the Nanotechnology Department, Southern Federal University (Rostov-on-Don, Russian Federation).

<https://orcid.org/0000-0001-9802-9335>
nvlyanguzov@sfedu.ru

Ilya Pankov, Cand. Sci. (Chem.), Lead Engineer of the Shared Use Center “High-Resolution Transmission Electron Microscopy”.

<https://orcid.org/0000-0001-5302-4792>
ipankov@sfedu.ru

Andrey A. Kokhanov, student, Southern Federal University (Rostov-on-Don, Russian Federation).

<https://orcid.org/0009-0003-6546-0710>
akokhanov@sfedu.ru

Received February 6, 2025; approved after reviewing March 11, 2025; accepted for publication March 17, 2025; published online December 25, 2025.